

## Light-Induced Melting of Colloidal Crystals in Two Dimensions

Erwin Frey,<sup>1</sup> David R. Nelson,<sup>1</sup> and Leo Radzihovsky<sup>2</sup>

<sup>1</sup>*Department of Physics, Harvard University, Cambridge, Massachusetts 02138*

<sup>2</sup>*Department of Physics, University of Colorado, Boulder, Colorado 80309*

(Received 18 May 1999)

We demonstrate that particles confined to two dimensions (2D) and subjected to a one-dimensional (1D) periodic potential exhibit a rich phase diagram, with both “locked floating solids” and smectic phases. The resulting phases and phase transitions are studied as a function of temperature and potential strength. We find reentrant melting as a function of the potential strength. Our results lead to universal predictions consistent with recent experiments on 2D colloids in the presence of a laser-induced 1D periodic potential.

PACS numbers: 64.70.Dv, 61.72.Lk, 64.70.Kb, 82.70.Dd

Landau’s order parameter expansion predicts that the direct transition from a solid to a liquid should *always* be first order [1]. In two dimensions (2D), however, fluctuations can suppress the transition temperature so far below its mean-field value that order parameter amplitude fluctuations (except in the form of topological defects) play no role, and Landau’s mean-field analysis is qualitatively wrong. In this case a two-stage melting process mediated by the unbinding of dislocations [2,3] and disclinations [3] provides an alternative scenario with two successive continuous phase transitions with an intermediate hexatic phase instead of a single direct first order transition. A periodic embedding medium for the 2D solid (e.g., a crystal substrate or a laser potential) leads to commensurability effects and engenders an enormous variety of interesting phenomena [4].

Colloids confined between glass plates [5,6] and paramagnetic colloidal systems [7] provide ideal model systems for experimental studies of 2D melting. In these systems individual particles can be imaged, allowing a direct observation of topological defects and measurement of real-space correlation functions. Murray *et al.* [5] and Zahn *et al.* [7] have given strong experimental evidence for a two-stage melting mechanism in such systems (because dislocations relax slowly, long equilibration times are required [5]). Chowdhury *et al.* [6] studied 2D colloidal suspensions subjected to a 1D periodic potential provided by the standing wave pattern of two interfering laser beams. They observed a phenomenon called “light-induced freezing,” a solidification driven by a commensurate laser potential. Our research is motivated by the recent work of Wei *et al.* [8], who reinvestigated this phenomenon and discovered *reentrant melting* upon gradually increasing the amplitude of the potential even farther.

Previous theoretical studies of this phenomenon have used density functional theory [9] which gives essentially the same results as Landau theory [6], namely, a change from first to second order critical behavior with increasing potential strength. Continuous melting is allowed because the external potential singles out density modes in one direction and the relevant Landau theory then con-

tains only even powers in the local Fourier components of the density  $\rho_{\mathbf{G}}(\mathbf{r}) = \exp(i\mathbf{G} \cdot \mathbf{r})$ . Unfortunately, the applicability of mean-field-like theories to problems with continuous symmetry in 2D is limited since these theories drastically underestimate the effect of fluctuations. Results from Monte Carlo simulations are inconclusive: Although earlier simulations [10] claimed to have found a tricritical point at intermediate laser intensities and reentrance, recent studies from the same laboratory [11] refute these results. We note that simulations with much larger numbers of particles have still not completely resolved the nature of 2D melting *without* an external potential [12].

In this Letter we take a different approach, building on concepts developed in the context of dislocation mediated melting theory [2,3]. We model the experimental system by a continuum elastic free energy  $F = F_{el} + F_p$ , where  $F_{el} = \frac{1}{2} \int d^2 r (2\mu u_{ij}^2 + \lambda u_{kk}^2)$  is the elastic energy associated with the colloidal displacement field  $\mathbf{u}(x, y)$  relative to the equilibrium position in the unconstrained solid characterized by the “bare” elastic constants  $\mu$  and  $\lambda$ . The quantity  $u_{ij} = \frac{1}{2}(\partial_i u_j + \partial_j u_i)$  is the 2D strain matrix. The effect of the laser potential with troughs running along the  $x$  axis is described by  $F_p = \int d^2 r U(y, u_y)$ , where  $U(y, u_y) = -U_0 a^{-2} \cos[\frac{2\pi}{d}(u_y - \delta y)]$ .  $U_0$  measures the strength of the laser potential and the mean colloidal spacing  $a$  is related to the particle density  $\rho$  by  $\rho = 2/\sqrt{3} a^2$ . A similar model was used to discuss modulated superconducting films in Ref. [4].

Let  $a'$  be the Bragg plane spacing for the orientation of the colloidal crystal (relative to the troughs) which produces the lowest free energy (see Fig. 1). Incommensurability between  $a$  and the distance between the troughs,  $d$ , is accounted for by the mismatch parameter  $\delta = a'/d - p$ , where  $p$  is the integer closest to  $a'/d$ .

For  $\delta = 0$ , we can write  $U(y, u_y) = -U_0 a^{-2} \cos[\mathbf{K}_p \cdot \mathbf{u}]$ , where  $\mathbf{K}_p = \frac{2\pi}{a'} p \mathbf{e}_y$  is a reciprocal lattice vector of the unperturbed system. If  $U_0 = 0$ , there are algebraic Bragg peaks in the structure function of the crystalline phase and  $M_{\mathbf{K}} \equiv \langle \rho_{\mathbf{K}} \rangle \sim 1/L \bar{\eta}_{\mathbf{K}}^{1/2} \rightarrow 0$  as the system size  $L \rightarrow \infty$ , where  $\bar{\eta}_{\mathbf{K}} = \frac{k_B T}{4\pi} \frac{3\mu + \lambda}{\mu(2\mu + \lambda)} \mathbf{K}^2$

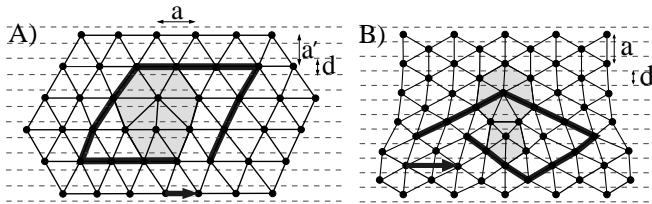


FIG. 1. Triangular lattice with lattice constant  $a$  subject to a periodic potential (maxima indicated by dashed lines) for two different relative orientations: (A)  $p_A d = a'_A$  with  $a'_A = \sqrt{3}a/2$  and  $p_A = 2$ ; (B)  $p_B d = a'_B$  with  $a'_B = a/2$  and  $p_B = 1$ . Also shown are low energy dislocations with Burgers vector  $\mathbf{b}$  parallel to the corrugation of the potential.

[3]. It is straightforward to show that  $M_{\mathbf{K}}$  then vanishes for small  $U_0$  as  $M_{\mathbf{K}} \sim |U_0|^{\overline{\eta}_{\mathbf{K}}/(4-\overline{\eta}_{\mathbf{K}})}$  [13]. In contrast,  $M_{\mathbf{K}}$  should always vanish *linearly* with  $U_0$  in the liquid and hexatic phases [5,7] of the unperturbed colloid. The laser potential will also induce long-range bond orientational order in  $\psi_6 = \langle e^{6i\theta(\mathbf{r})} \rangle$  [14]. The bond order parameter  $\psi_6$  vanishes linearly with  $U_0$  in the liquid, vanishes like a power of  $U_0$  in the hexatic phase [ $\psi_6 \sim |U_0|^{6\overline{\eta}_6/(4-\overline{\eta}_6)}$ , where  $\overline{\eta}_6$  is the exponent describing the algebraic decay of bond order], and approaches a nonzero constant as  $U_0 \rightarrow 0$  in the solid phase.

In our analysis of larger values of  $U_0$ , we shall also focus on the commensurate case ( $\delta = 0$ ), where the spacing  $a'$  of the lattice planes parallel to the troughs equals an integer  $p$  times  $d$ . In Fig. 1, two particularly interesting orientations, denoted A and B, of the colloidal crystal and laser potential are shown. Only dislocations with a Burgers vector parallel to the troughs have the usual logarithmically divergent energy. In orientation A, four of the six fundamental Burgers vectors are disfavored by the potential, which requires that they be attached to a semi-infinite discommensuration string [4]. In orientation B, all *six* fundamental Burgers vectors are disfavored. The lowest energy Burgers vector parallel to the troughs has length  $\sqrt{3}a$ . At sufficiently low temperatures, the laser potential is always relevant [3], leaving massless phonon displacements  $u_x$  along the troughs with massive out-of-valley displacements  $u_y$ . We call this ordered phase a “locked floating solid” (LFS), reflecting its resistance to strains associated with  $u_y$  and its ability to accommodate strains in  $u_x$ . In reciprocal space, the LFS is characterized by a structure function  $S(\mathbf{q})$  with a row of  $\delta$ -function Bragg peaks at  $G_y^{(n)} = 2\pi \frac{n}{d}$  ( $n \in \mathbb{Z}$ ) along the  $q_y$  axis and power law Bragg peaks off this axis (see Fig. 2).

Upon integrating out the massive  $u_y$  modes and using standard renormalization group methods [3,15] to eliminate bound dislocation pairs in the LFS phase, we are left with a free energy with temperature and potential strength dependent *effective* elastic constants,

$$F_{\text{LFS}} = \frac{1}{2} \int d^2 r \{ K_{\text{eff}} (\partial_x u_x)^2 + \mu_{\text{eff}} (\partial_y u_x)^2 \}. \quad (1)$$

Because only dislocations with Burgers vectors parallel to the troughs are important, the physics is described by

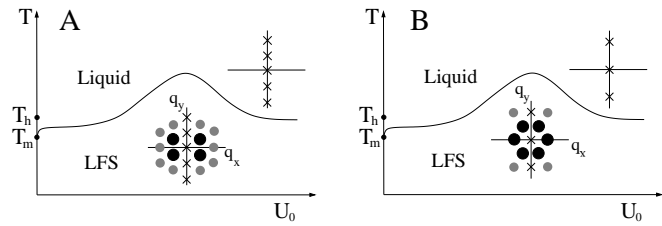


FIG. 2. Schematic  $p = 1$  phase diagram for orientations A and B. Insets: schematic structure functions in the various phases. The  $\times$ 's indicate delta-function Bragg peaks and circles indicate algebraic peaks.  $T_h$  indicates the transition temperature from the hexatic to the liquid phase at  $U_0 = 0$ .

an anisotropic scalar Coulomb gas or, equivalently, an anisotropic 2D XY model. For  $p$  smaller than a critical value  $p_c$  we find that the LFS melts with increasing temperature at

$$k_B T_m = \frac{\sqrt{K_{\text{eff}} \mu_{\text{eff}}}}{8\pi} b^2, \quad (2)$$

via an unbinding of dislocations with Burgers vectors  $\mathbf{b} \parallel \mathbf{e}_x$  *before* the laser potential which gives the mass to the  $u_y$  modes, becomes irrelevant (see below). For  $T < T_m$  the correlation function  $C_{\mathbf{G}}(\mathbf{r}) = \langle \rho_{\mathbf{G}}(\mathbf{r}) \rho_{\mathbf{G}}^*(0) \rangle$  for reciprocal lattice vectors with  $G_x \neq 0$  shows power law decay  $C_{\mathbf{G}}(\mathbf{r}) \sim |(\mu_{\text{eff}}/K_{\text{eff}})^{1/2} x^2 + (K_{\text{eff}}/\mu_{\text{eff}})^{1/2} y^2|^{-\eta_{\mathbf{G}}/2}$ . The structure function is singular,  $S(\mathbf{q}) \sim 1/|\mathbf{q} - \mathbf{G}|^{2-\eta_{\mathbf{G}}}$ , near the reciprocal lattice vector  $\mathbf{G}$  [3]. The exponents  $\{\eta_{\mathbf{G}}\}$  are given in terms of the elastic constants by  $\eta_{\mathbf{G}} = k_B T G_x^2 / 2\pi \sqrt{K_{\text{eff}} \mu_{\text{eff}}}$ .

Unlike conventional 2D melting [3],  $\eta_{\mathbf{G}}$  is *universal* at the melting transition, and given by  $\eta_{\mathbf{G}}^* = (\mathbf{G} \cdot \mathbf{b} / 4\pi)^2$ , where  $\mathbf{b}$  is the smallest allowed Burgers vector in the trough direction [15]. For orientation A,  $b = a$  and the exponent characterizing the algebraic order in the off-axis peaks (see insets of Fig. 2) closest to the  $q_y$  axis is  $\eta_{\mathbf{G}}^* = 1/4$ ; for the next row of peaks with  $G_x = 4\pi/a$ , one gets  $\eta_{\mathbf{G}}^* = 1$ , consistent with the algebraic decay observed in Ref. [8]. For orientation B,  $b = \sqrt{3}a$  and the six quasi Bragg peaks closest to the origin have *different* power laws; peaks on the  $x$  axis have  $\eta_{\mathbf{G}}^* = 1$ , whereas the four off-axis peaks have  $\eta_{\mathbf{G}}^* = 1/4$ . Just above the melting temperature, we expect diverging translational correlation lengths (defined by the widths of Lorentzian peaks in the structure function) parallel and perpendicular to the troughs  $\xi_x \sim \xi_y \sim \exp[\text{const}/|T - T_m|^{1/2}]$ .

To obtain the melting curve as a function of  $U_0$  we calculate  $K_{\text{eff}}$  and  $\mu_{\text{eff}}$  and use Eq. (2). We start from a microscopic model with a screened repulsive Coulomb interaction [16]  $V(r) = V_0 a \exp(-\kappa r)/r$ , where the screening length  $\kappa^{-1}$  is typically much smaller than  $a$  and  $V_0$  depends on the dielectric constant,  $\kappa$ , and the sphere radius [8]. In such a dilute limit the two Lamé coefficients are equal,  $\lambda = \mu$ . Hence the Kosterlitz-Thouless melting temperature in the absence of a laser potential ( $U_0 = 0$ ) is simply given by [3]  $k_B T_m^0 = \mu a^2 / 6\pi$ . In the opposite limit of *infinite* potential strength the effective free energy simplifies to Eq. (1) with  $K_{\text{eff}} = 3\mu$  and  $\mu_{\text{eff}} = \mu$ .

Using Eq. (2), this gives  $k_B T_m^\infty = \sqrt{3} \mu a^2 / 8\pi \approx 1.3 k_B T_m^0$ . One might have thought that the melting temperature simply increases monotonically with  $U_0$  from  $T_m^0$  to  $T_m^\infty$ . It turns out, however, that fluctuations in the  $u_y$  modes caused by lowering the potential strength from infinity typically *increase* the melting temperature. To see this, we integrate out the  $u_y$  modes using the screened Coulomb potential; to leading order in  $k_B T / U_0$  and  $V_0 e^{-\kappa a} / U_0$ , we find (for orientation A) [15]

$$\mu_{\text{eff}} \approx \mu \left\{ 1 + \frac{9(\kappa a)^2}{64\pi^2} \left( 1 + \frac{17}{3\kappa a} \right) \frac{k_B T}{p^2 U_0} \right\}, \quad (3)$$

$$K_{\text{eff}} \approx K \left\{ 1 + \frac{(\kappa a)^2}{64\pi^2} \left( 1 - 8\nu - \frac{23 + 104\nu}{3\kappa a} \right) \frac{k_B T}{p^2 U_0} \right\}, \quad (4)$$

where  $\nu = V_0 e^{-\kappa a} / k_B T$ ,  $\mu = \frac{3}{8} \nu k_B T \kappa^2$ , and  $K = 3\mu$ . Lowering the potential strength  $U_0$  always increases the shear modulus, whereas the behavior of the compressional modulus depends on the magnitude of  $\nu$  and  $\kappa a$ . When combined with Eq. (2), these expressions imply that the melting temperature  $T_m$  increases with decreasing  $U_0$  for  $\kappa a \gtrsim 5.6$  (in Ref. [8],  $\kappa a \approx 10$ ),

$$T_m \approx T_m^\infty \left\{ 1 + \frac{5[(\kappa a)^2 - 31]}{64\pi^2} \left( 1 + \frac{13}{3\kappa a} \right) \frac{k_B T_m^\infty}{p^2 U_0} \right\}, \quad (5)$$

thus implying reentrant melting for a band of tempera-

tures as a function of potential strength (see Fig. 2). For a more precise estimate of the phase boundary, one would also need to determine the renormalization of the effective elastic constants by phonon nonlinearities and by bound dislocation pairs. In general, however, one expects only small downward renormalizations with increasing temperature [17] which will not affect the existence of reentrant melting. For small  $U_0$ , we find that the melting curve has a universal shape  $T_m(U_0) - T_m(0) \sim [\ln(k_B T_m / U_0)]^{-1/\bar{\nu}}$  with  $\bar{\nu} \approx 0.36963 \dots$

We now discuss the topology of the phase diagram for larger values of the commensurability parameter  $p$ . As illustrated in Fig. 3, for  $p > p_c$  a floating solid (FS) with *two* soft phonon modes [3] can intervene (barring a direct first order transition) between the LFS and the liquid phase. To determine  $p_c$ , one must calculate the thermal renormalization of the laser potential, defined by  $U_0(s) = U_0 s^2 \exp[-\frac{1}{2} K_p^2 \langle u_y^2 \rangle] \equiv U_0 s^{\lambda_p}$ , where  $\lambda_p$  is a renormalization group eigenvalue and the subscript “>” indicates that the  $u_y$  modes are integrated over a momentum shell  $[\Lambda/s, \Lambda]$ . The potential becomes irrelevant at long wavelengths whenever  $\lambda_p < 0$ . The thermal average over the  $u_y$  modes requires an effective elastic long wavelength free energy appropriate to the FS phase. Because the laser potential breaks rotational symmetry, this coarse-grained free energy contains *six* independent elastic constants,

$$F_{\text{FS}} = \int d^2 r \left\{ 2\mu u_{xy}^2 + \frac{1}{2} \lambda_{xx} u_{xx}^2 + \frac{1}{2} \lambda_{yy} u_{yy}^2 + \lambda_{xy} u_{xx} u_{yy} + 2\gamma \theta^2 + 2\alpha \theta u_{xy} \right\}, \quad (6)$$

where  $\theta = \frac{1}{2}(\partial_x u_y - \partial_y u_x)$  is the local rotation angle induced by the phonon displacements. The resulting expression for  $\lambda_p$  is rather complicated, with an implicit dependence on the strength of the laser potential and the temperature [15]. However, a useful estimate results from neglecting the effect of the substrate on the elastic coefficients and considering an isotropic elastic free energy. For orientation A, one finds [3]  $\lambda_p = 2 - \frac{4\pi}{3} \frac{k_B T}{\mu a^2} p^2$  with the effective elastic constant  $\bar{\mu} = 2\mu(2\mu + \lambda)/(3\mu + \lambda)$ . In the dilute limit  $\kappa a \gg 1$ , relevant for many colloidal systems, we have  $\mu = \lambda$  and the eigenvalue is negative for  $T > T_p^{\text{dil}}$ , with  $\bar{\mu} = 3\mu/2$  and  $k_B T_p^{\text{dil}} \approx 9\mu a^2 / 4\pi p^2$ . When compared with the melting temperature of the LFS phase in the same limit of  $\kappa a \gg 1$  for weak potentials,  $k_B T_m^0 \approx \mu a^2 / 6\pi$ , we find that a window of the FS phase exists for  $p > p_c \approx 3\sqrt{3}/2 \approx 3.7$  for orientation A [18]. Note, however, that  $p_c$  is not a universal constant but implicitly depends on the strength of the potential,  $p_c(U_0)$ .

For intermediate commensurate densities  $1 < p < p_c$ , no FS phase exists, and the dislocation unbinding transition discussed above melts the LFS to a locked smectic (LSm) phase. In the LSm phase the potential is relevant and only one out of  $p$  possible troughs is preferentially

occupied by the colloidal particles. At higher temperatures an Ising transition ( $p = 2$ ) (more generally,  $p$ -state clock model [19]) takes the system to a modulated liquid phase. We expect the same type of reentrant behavior for the LFS-LSm phase boundary as discussed above for  $p = 1$ . However, the LSm-liquid phase boundary should depend more weakly on the potential strength: Since the shear modulus is zero in the LSm phase the reentrance mechanism discussed above does not apply here.

For  $p > p_c$  the laser potential becomes irrelevant *before* the LFS melts (via a rougheninglike transition),

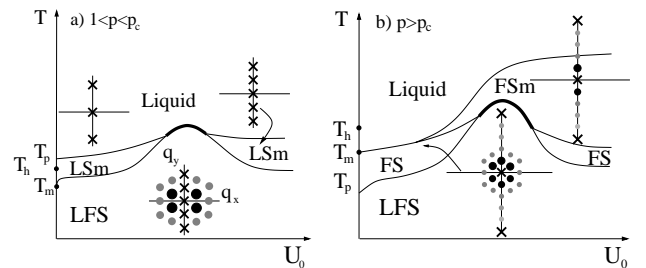


FIG. 3. Schematic phase diagrams for (a)  $1 < p < p_c$  and (b)  $p > p'_c > p_c$  (for orientation A). Heavy lines indicate phase transitions which are most likely of first order. Insets: schematic structure functions.

leading to the uniaxially anisotropic FS described by  $F_{\text{FS}}$  [Eq. (6)]. Melting of this uniaxial solid (with  $\gamma = \alpha = 0$ ) has been studied in detail by Ostlund and Halperin [20]. Because of the uniaxial anisotropy, there are two different types of dislocations: type-I dislocations with Burgers vector along a reflection symmetry axis of the solid, and type-II dislocations at angles  $\pm\phi_0$  with respect to this axis. The laser potential in Fig. 1A is oriented in such a way that type-I dislocations are parallel to the troughs of the potential, interact more weakly, and will therefore unbind first. This “type-I” melting transition leads to a “floating smectic” phase (FSm) stabilized by the potential such that it retains quasi-long-range order in  $\rho_{\mathbf{G}} = \exp[i\mathbf{G} \cdot \mathbf{u}]$  for  $\mathbf{G} = 2\pi\mathbf{e}_y/pd$ . We expect that a FSm phase intervenes between a FS and the liquid if  $p$  is sufficiently large ( $p \geq p_c^I = 4$  [19]).

The novelty of this FS-FSm type-I melting is that, in contrast to the similar melting of the LFS, the destruction of translational order in  $u_x$  by dislocations takes place in the presence of a coupled “spectator” massless phonon mode  $u_y$ . To analyze this transition we proceed in the standard way [3,19] by introducing type-I dislocations into the elastic free energy and performing a duality transformation on the resulting Coulomb gas Hamiltonian to convert it into a modified Sine-Gordon model,

$$H = \int d^2 r \left\{ \frac{|\nabla h|^2}{2K_I} - g \cos[a(h + i\psi)] \right\} + F_{\text{FS}}[\boldsymbol{\phi}]. \quad (7)$$

Here  $h(x, y)$  is a dummy field which when integrated out in  $\exp(-H/k_B T)$  gives rise to a scalar Coulomb gas with interaction strength proportional to  $K_I$ . The quantity  $\boldsymbol{\phi}$  is the single valued part of the displacement fields,  $\psi(\mathbf{q}) = [\lambda_{xy}q_y^2 - (\mu - \gamma)q_x^2]u_y(\mathbf{q})/q^2$  and  $g \equiv 2e^{-E_c/k_B T}$  with  $E_c$  the core energy of type-I dislocations. The melting temperature can be determined from the condition that the renormalization group eigenvalue of  $g$  vanishes,

$$k_B T_{\text{FS-FSm}} = \frac{a^2}{8\pi} \left( \sqrt{\lambda_{xx}\mu_-} - c \frac{\mu^2}{\sqrt{\mu + \lambda_{yy}}} \right), \quad (8)$$

with suitable renormalized elastic constants. Here  $\mu_{\pm} = \mu + \gamma \pm \alpha$ , and  $c$  is a dimensionless function of ratios of the FS elastic constants [15]. The effect of the spectator phonon modes is to reduce the melting temperature. Just below  $T_{\text{FS-FSm}}$  we find for the renormalized stiffness  $K_I^R(T) \approx K_I^R(T_{\text{FS-FSm}})[1 + \text{const}(T_{\text{FS-FSm}} - T)^{1/2}]$ . Above the melting temperature  $K_I$  is zero, type-I dislocations are unbound, and at long length scales the elastic free energy describing the FSm phase is of the form  $F_{\text{FSm}} = \frac{1}{2} \int d^2 r \{ B_x (\partial_x u_y)^2 + B_y (\partial_y u_y)^2 \}$  with  $B_x \approx [4\gamma\mu - \alpha^2]/(\mu + \gamma - \alpha)$  and  $B_y \approx \lambda_{yy} - \lambda_{xy}^2/\lambda_{xx}$ . Note that  $B_x$  vanishes for  $\gamma = \alpha = 0$  as one would expect for a rotationally invariant 2D smectic. The structure factor in the FSm phase exhibits power law singularities at reciprocal lattice vectors  $\mathbf{G}_n = 2\pi n\mathbf{e}_y/pd$  (for

$n \neq p$ ), with an exponent  $\eta_{\text{FSm}} = k_B T G_n^2 / 2\pi \sqrt{B_x B_y}$ . The FSm phase melts via a second dislocation unbinding transition when  $\eta_{\text{FSm}} \geq 1/4$ .

We have only discussed potentials which are commensurate with the colloidal crystal. Sufficiently large incommensurability favors the discommensurations attached to Burgers vectors with an unfavorable orientation relative to the troughs [4], and leads to a large variety of phase transitions as a function of density at fixed trough spacing which we will discuss in a future publication.

It is a pleasure to thank B. I. Halperin for helpful discussions, and C. Bechinger and P. Leiderer for communicating unpublished results. This work has been supported by the DFG through a Heisenberg Fellowship (Fr 850/3-1) (E. F.), by the NSF through Grant No. DMR-9714725 (D. R. N.), Harvard’s MRSEC Grant No. DMR98-09363 (D. R. N.), Grant No. DMR-9625111 (L. R.), University of Colorado’s MRSEC Grant No. DMR-9809555 (L. R.), and by the A.P. Sloan and Packard Foundations (L. R.).

- 
- [1] L. D. Landau, Phys. Z. Sowjet. **11**, 26 (1937); see also S. Alexander and J. McTague, Phys. Rev. Lett. **41**, 702 (1978).
  - [2] J. M. Kosterlitz and D. J. Thouless, J. Phys. C **6**, 1181 (1973); A. P. Young, Phys. Rev. B **19**, 1855 (1979).
  - [3] B. I. Halperin and D. R. Nelson, Phys. Rev. Lett. **41**, 121 (1978); D. R. Nelson and B. I. Halperin, Phys. Rev. B **19**, 2457 (1979).
  - [4] For a review see, e.g., V. Pokrovsky *et al.*, in *Solitons*, edited by S. Trullinger *et al.* (North-Holland, Amsterdam, 1986).
  - [5] C.-A. Murray *et al.*, Phys. Rev. B **42**, 688 (1990).
  - [6] A. Chowdhury *et al.*, Phys. Rev. Lett. **55**, 833 (1985).
  - [7] K. Zahn *et al.*, Phys. Rev. Lett. **82**, 2721 (1999).
  - [8] Q.-H. Wei *et al.*, Phys. Rev. Lett. **81**, 2606 (1998).
  - [9] J. Chakrabarti *et al.*, Phys. Rev. Lett. **73**, 2923 (1994).
  - [10] J. Chakrabarti *et al.*, Phys. Rev. Lett. **75**, 2232 (1995).
  - [11] C. Das *et al.*, cond-mat/9902006, 1999.
  - [12] See, e.g., K. Bagchi *et al.*, Phys. Rev. E **53**, 3794 (1996).
  - [13] For  $\eta_{\mathbf{K}} > 2$ ,  $M_{\mathbf{K}}$  vanishes linearly with  $U_0$ , with a singular correction.
  - [14] See, e.g., L. Balents and D. R. Nelson, Phys. Rev. Lett. **73**, 2618 (1994).
  - [15] L. Radzihovsky, E. Frey, and D. R. Nelson (unpublished).
  - [16] We do not have to take into account an attractive component in the pair potential [see, e.g., J. Crocker and D. Grier, Phys. Rev. Lett. **77**, 1897 (1996)] since in Ref. [8] both the interparticle distance and the spacing between the plates are too large for those effects to be relevant.
  - [17] D. S. Fisher, Phys. Rev. B **26**, 5009 (1982); D. S. Fisher, B. I. Halperin, and R. Morf, Phys. Rev. B **20**, 4692 (1979).
  - [18] For the geometry in Fig. 1B dislocations with a larger Burgers “charge,”  $\mathbf{b} = \sqrt{3}a$ , unbind. Hence  $k_B T_m^0 \approx \frac{\mu a^2}{2\pi}$  and  $k_B T_p^{\text{dil}} \approx \frac{3\mu a^2}{4\pi p^2}$  and thus  $p_c \approx \sqrt{3/2} \approx 1.2$ .
  - [19] J. V. José *et al.*, Phys. Rev. B **16**, 1217 (1977).
  - [20] S. Ostlund and B. I. Halperin, Phys. Rev. B **23**, 335 (1981).